

Prediction and optimization of load and torque in ring rolling process through development of artificial neural network and evolutionary algorithms

Hamid Reza Rohani Raftar^a, Ali Parvizi^{b,*}

^a Department of Mechanical and Aerospace Engineering, Science and Research Branch, Islamic Azad University, Tehran, Iran

^b Assistant Professor, School of Mechanical Engineering, College of Engineering, University of Tehran, Tehran, Iran

ARTICLE INFO

Article history:

Received

Received in revised form

Accepted

Available online

Keywords:

Artificial neural network

FEM

Genetic

Optimization

Ring rolling

ABSTRACT

Developing artificial neural network (ANN), a model to make a correct prediction of required force and torque in ring rolling process is developed for the first time. Moreover, an optimal state of process for specific range of input parameters is obtained using Genetic Algorithm (GA) and Particle Swarm Optimization (PSO) methods. Radii of main roll and mandrel, rotational speed of main roll, pressing velocity of mandrel and blank size are considered as input parameters. Furthermore, the required load and torque in ring rolling process are taken into account as process outputs. Various three dimensional finite element simulations are performed for different sets of process variables to achieve preliminary data for training and validation of the neural network. Besides, the finite element model is approved via comparison with the experimental results of the other investigators. The Back Propagation (BP) algorithm is considered to develop Levenberg–Marquardt feed-forward network. Additionally, Model responses analysis is carried out to improve the understanding of the behavior of the ANN model. It is concluded that results of ANN predictions have an appropriate conformity with those from simulation and experiments. Moreover, GA and PSO methods have been implemented to obtain the optimal state of process while their outcomes have been also compared.

1. Introduction

Ring rolling is regarded as a versatile metal-forming process for manufacturing seamless annular forgings which are accurately dimensioned and have circumferential grain flow. Ring rolling generally requires less input material than the alternative forging methods, and is applicable in production of any quantity. Annular components can be ring rolled from any forgeable material. To obtain wide-ranging quality outcomes from ring rolling process, it is efficient to implement the process parameters in the optimum condition. The angular velocity of main roll (N) and the pressing velocity of the mandrel (V) are known as two significant parameters should be evaluated in the ring rolling process. Moreover, the radii of the mandrel (R_2) and main roll (R_1) as well as the ring volume, i.e. the current radius and thickness of the ring, are the geometrical process parameters ought to be considered in this process [1].

The past decades have seen the rapid development in the ring rolling process for manufacturing seamless rings in a wide geometrical range. An upper bound method has been applied by Parvizi and Abrinia [2] to find the ring rolling power and force. Their study illustrated that the required force for implementation of the process increased slowly, while the ring mean radius

increases. Yang and Ryou [3] carried out some experiments in order to investigate the ring rolling process and determine the relationship between torque and load.

Finite element method (FEM) is an efficient technique to analyze the metal forming processes. Over the years, some FEM analyses have been conducted by numerous researchers to predict the results of ring rolling process. Employing ABAQUS dynamic explicit code, Zhou et al. [4] developed 3D elastic–plastic and coupled thermo-mechanical FE model of radial–axial ring rolling. The influence of the rolls sizes on quality of rolled ring was addressed by the researchers.

Artificial neural network (ANN) is a computational model established based on the characteristics of natural neural network and widely applied for its ability to estimate the results according to the numerous number of input data [5]. Based on its distinguished features to learn from samples and make use of the modifications to the subsequent parameters, such powerful information processing system can be considered as an effective technique to perform computation in different fields such as metal forming processes. An ANN model was designed by Altinkaya et al. [6] to find optimum parameters values for rail rolling process. Those studies presented that instead of using complex methods and

* Corresponding author. Tel.: +98 21 61119953; aliparvizi@ut.ac.ir

analytical equations, ANNs are able to be implemented for controlling the parameter values required for product design in the rail rolling process.

Optimization methods might be regarded as efficient means to improve the processes such as metal forming and lead to more optimum products. Investigating the optimum state in extrusion process, Sharififar and Mousavi [7] applied genetic algorithm to accomplish the lowest magnitude of extrusion force. An experimental investigation into optimization of EDM process factors for Inconel 718 using genetic algorithm was carried out by Moghaddam and Kolahan [8]. They found out how to arrange the parameters of EDM process for escalating the quality of final product. During the last two decades, the PSO algorithm has been exploited in numerous areas of process optimizations. Jalilrad et al. [9] implemented the particle swarm optimization technique to comprehend what situation is able to be regarded as an optimal design of shell-and-tube heat exchanger. Their present method managed to gain appropriate parameters for optimization of the process.

Surveying the literature indicates that the investigation regarding the effects of process factors on minimizing the load and torque in ring rolling process with ANN, GA and PSO considerations has not been reported. Developing an ANN model for a ring rolling process to predict the correct rolling force and torque as well as defining an optimal state of the process using GA method for different process conditions are the goals of the current study. Data considered as a basis for training and validation of the neural network is achieved by three-dimensional finite element simulation of the process. Taguchi method is used to design the combination of the factors required for studying the influence of the input parameters, i.e. R_1 , R_2 , V , N and blank size of ring. The results indicate that ANN model is so successful in estimation of the roll force and torque and optimized setting parameters are obtained by GA and PSO methods.

2. Basic theory

The principal difference between ring rolling and normal flat rolling of sheets is the actual fact that the mandrel is of smaller radius, main roll, and advancing incrementally and constantly toward a rotating main roll of larger radius. Mechanical model of ring rolling is shown in Fig. 1.

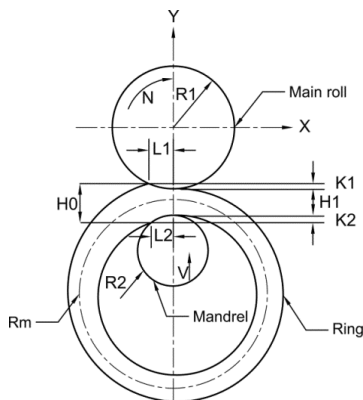


Fig. 1. Mechanical model of ring rolling process

The projected contact length between the ring and the main roll L_1 and that between the ring and the mandrel L_2 can be achieved from the following relationships [10]:

$$L_1 = \sqrt{R_1^2 - \frac{\left[(R_m + H_1 / 2 + k_1)^2 - R_1^2 \right]^2}{2(R_1 + H_1 / 2 + R_m)}} \tag{1}$$

$$L_2 = \sqrt{R_2^2 - \frac{\left[(R_2^2 + (H_1 / 2 + R_2 - R_m)^2 \right]^2}{2(H_1 / 2 + R_2 - R_m)}} \tag{2}$$

$$\frac{L_1}{L_2} = \frac{k_2}{k_1 [1 + H_0 / (2R_m)]} \tag{3}$$

$$H_0 = \frac{1}{2} \left[\frac{V}{W \pi R_m} + \frac{60V_p [R_m + V / (4W \pi R_m)]}{R_1 N_D} \right] \tag{4}$$

$$H_1 = \frac{1}{2} \left[\frac{V}{W \pi R_m} - \frac{60V_p [R_m + V / (4W \pi R_m)]}{R_1 N_D} \right] \tag{5}$$

$$H_0 - H_1 = k_1 + k_2 \tag{6}$$

Where H_0 and H_1 are ring thicknesses at the entrance and exit, respectively, V is the volume of the ring, W is the width of the ring, R_m is the mean radius of the current ring, V_p is the feed speed at the mandrel, R_1 is the radius of the main roll, R_2 is the radius of the pressure roll, N_D is the rotational speed of the main roll in rpm and k_1+k_2 is the feed per revolution of the ring.

3. Finite element simulation

The unsteady state nature of the process which includes the continuously varying deforming zone as well as the unsymmetrical condition of the geometry with the complicated boundary conditions are some complexities in developing the finite element simulation of the ring rolling process. Applying DEFORM software, three-dimensional dynamic explicit analysis was considered to perform the simulation. The model of the process is shown in Fig. 2 wherein the guide rolls are not considered for simplification.

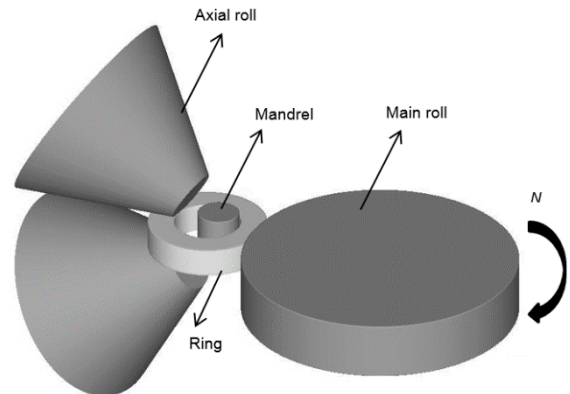


Fig. 2. 3D FE model of the process

For rigid-plastic finite element analysis, the functional is given by [11]:

$$\Pi = \int_V \bar{\sigma} \dot{\bar{\epsilon}} dV + \int_V \lambda \dot{\epsilon}_v dV - \int_{S_F} \mathbf{F} \cdot \mathbf{u} dS - \int_{S_c} \left(\int_0^{|\mathbf{v}_r|} \mathbf{F}' \cdot d\mathbf{V}_r \right) dS \quad (7)$$

where $\bar{\sigma}$ is the effective stress, $\dot{\bar{\epsilon}}$ is the effective strain rate, λ is Lagrangian multiplier, ϵ_v is the volumetric strain rate, \mathbf{F} is the traction prescribed over the surface S_f , \mathbf{V} is the velocity vector, \mathbf{V}_r is the relative velocity and \mathbf{F}' is the velocity-dependent frictional stress over the interface surface S_c developed by Chen and Kobayashi [12] to treat a neutral point problem. \mathbf{F}' is given by

$$\mathbf{F}' = -m_f k \left[\frac{2}{\pi} \tan^{-1} \left(\frac{|\mathbf{V}_r|}{\alpha} \right) \right] \frac{\mathbf{V}_r}{|\mathbf{V}_r|} \quad (8)$$

Where K the yield is shear stress, m_f is the friction factor and α is a constant several orders of magnitude smaller than the roll velocity.

The following features were taken into account in developing the FE model:

1. The main roll, mandrel and axial rolls were assumed to be rigid.
2. The feed speed of the mandrel and angular velocity of main roll are constant.
3. The direction of mandrel linear movement as well as the rotational directions of main and axial rolls were considered as free and the other freedoms were constrained.
4. To avoid the huge computation time and convergence problem, the dynamic explicit FE solution was taken into account.
5. ALE finite element formulation was used to control the mesh distortion during the process. Thus, fine mesh was assigned to the roll gap as a main deformation region and coarse mesh was utilized in the other regions. Having this manner, the calculation time was significantly decreased and the computational accuracy was confirmed. Schematic illustration of the mesh model in cross section of ring as well as the whole ring is demonstrated in Fig. 3. Specification of mesh system is also provided in Table 1.
6. The constant shear friction model ($\tau = mk$) was assumed to simulate the friction on the interaction surfaces between ring and the rolls. Taking into account the hot rolling process, the friction coefficient was considered to be 0.7.

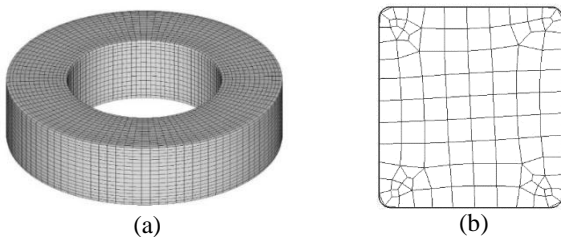


Fig. 3. Schematic of the mesh system for (a) ring (b) Cross section of ring

Table 1. Specification of mesh model

Number of 2D elements (in cross section area)	122
Number of revolving sections	100
Number of 3D elements	12200
Total number of node	15400

The SAE-AISI 1045 steel was selected as blank material whose density, Young's modulus and Poisson ratio are 7870 kgm^{-3} , 200 GPa and 0.29, respectively. The process was simulated at 1000°C . The constitutive model proposed by Johnson and Cook [13] was employed for material behavior as follows

$$\bar{\sigma} = \left[A + B (\bar{\epsilon})^n \right] \left[1 + C \ln \left(\frac{\dot{\bar{\epsilon}}}{\dot{\bar{\epsilon}}_0} \right) \right] \left[1 - \left(\frac{T - T_{room}}{T_{melt} - T_{room}} \right)^m \right] \quad (9)$$

where $\bar{\epsilon}$, $\dot{\bar{\epsilon}}$ and $\dot{\bar{\epsilon}}_0$ are plastic strain, plastic strain rate (s^{-1}) and the reference plastic strain rate (s^{-1}), respectively. Coefficient A and B are yield strength (MPa) and hardening modulus (MPa), respectively. Moreover, C , n , and m are strain rate sensitivity coefficient, hardening coefficient and thermal softening coefficient, respectively. In addition, T , T_{melt} and T_{room} are temperature of the workpiece material ($^\circ\text{C}$), melting temperature of the workpiece material ($^\circ\text{C}$) and room temperature ($^\circ\text{C}$), respectively. Moreover, Flow stress of AISI 1045 in low and high strain rate compression tests at various temperatures is illustrated in Fig. 4 [14].

The results of Deform software that represent the deformed geometry and stress contours are illustrated in Fig. 5.

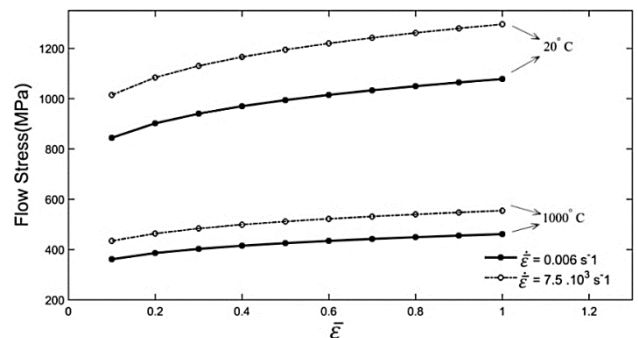


Fig. 4. stress-strain curve for AISI 1045 in low and high strain rate at various temperatures [14]

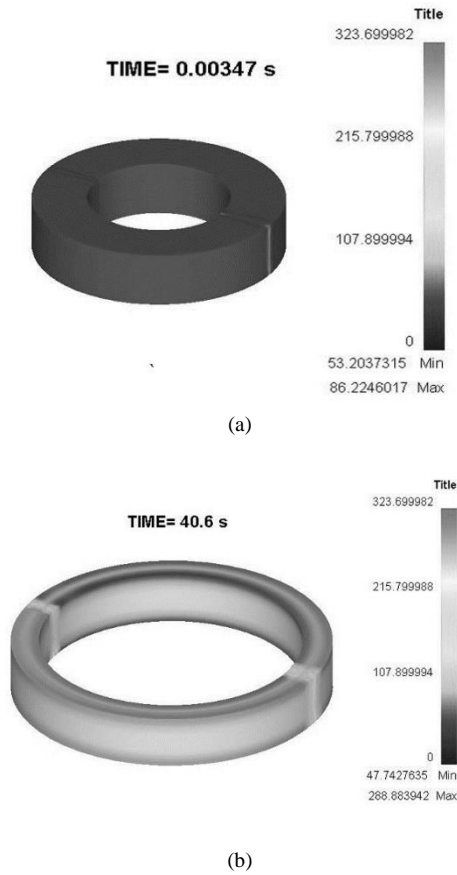


Fig. 5. the deformed geometry and stress contours (a) in the first step of simulation (b) in the last step of simulation

3.1 Verification of model

To verify the accuracy of present FE model, the experimental results of [1] for rolling load and torque were taken into account. Therefore, the same process parameters of [1], as given in Table 2, were used for hot ring rolling simulation.

Table 2. Experimental hot ring rolling parameters applied in the simulation

R ₁ (mm)	R ₂ (mm)	N (RPM)	V _p (mm/s)	OD (mm)	ID (mm)	W (mm)
275	45	47	0.7	215	120	52

The results of load and torque concerning ring rolling process obtained from present FE simulation and experiments of [1] are compared in Fig. 6. It is obvious that there exists an appropriate agreement between both results while the root mean square of differences between the load and torque results are about 1% and 8%, respectively. Consequently, the FE model was verified in order to simulate the ring rolling process.

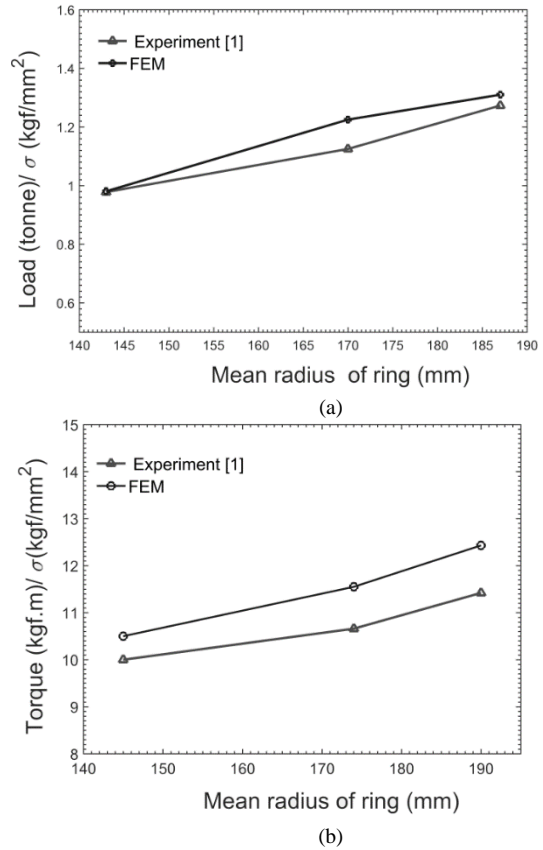


Fig. 6. Comparison between FE and experimental results for rolling (a) load (b) torque for different mean radius of ring

4. Artificial neural network model

An ANN is an information-processing scheme that has specific ability characteristics in common with biological neural networks. A neural network involves enormous number of simple processing elements called neurons. Each neuron is connected to the other neurons by means of directed communication links with a distinct associated weight. The weights denote information being used by the network to solve a problem [5]. A multilayer neural network which involves an input layer, one or more hidden layers, and an output layer is able to approximate an arbitrary function with a specified accuracy.

Every layer holds a definite number of processing neurons (elements) that are coupled by connection links with modifiable weights. These weights are renewed during the training process, most widely through the back-propagation learning algorithm by giving the neural network with instances of input-output sets displaying the relationship that network is trying to learn. The output of every neuron is calculated by multiplying its inputs by a weight vector, summing the outcomes, and using an activation function to the sum as follows [15]:

$$y = f \left[\sum_{k=1}^n X_k W_k + b_k \right] \quad (10)$$

Where n is the number of inputs, X_k is the input cost received from the preceding layer neuron, b_k is the bias of the elements, W_k is the corresponding weight of each linking and f is the activation function that is applied for limiting the amplitude of the elements output.

Through training, Q groups of input and output data are given to the artificial neural network. An iterative process modifies the weights so that the outputs (o_k) based on the input arrangements will be as close as possible to their respective desired output patterns (d_k). Considering a neural network with k that is the total number of outputs, the mean square error (MSE) function is to be minimized [16]:

$$MSE = \frac{1}{Q \times K} \times \sum_{q=1}^Q \sum_{k=1}^K [d_k(q) - O_k(q)]^2 \quad (11)$$

The back-propagation algorithm is most commonly utilized to minimize MSE by adapting the weights of the connection links [17].

4.1. Input and output parameters

The performance of neural network relies on the amount of data used for training. In other words, an influential neural network model requires an adequately large amount of accurate data. Considering a large number of parameters, the Taguchi's method

is employed to perform design of inputs for simulation runs. Radii of main roll and mandrel, rotational speed of main

roll, pressing velocity of mandrel and blank size were taken into account for independent input parameters. Taking into account four factors with three levels and one factor with two levels, as illustrated in Table 3, 54 simulation runs that result into the training data were designed for a mixed-level using Minitab statistical software. Table 4 indicates 54 sets of data were used to build the FE models for load and torque calculations.

Table 3. Level determination of various process variables

Factors	Levels		
	1	2	3
R ₁ (mm)	250	275	300
R ₂ (mm)	37.5	45	55
N _D (RPM)	35	47	60
V _p (mm/s)	0.5	0.7	0.9
Blank size (mm)	215×120×52	304×164×54	----

Table 4. 54 different condition arrays for FE simulation designed based on Taguchi method

No.	Blank size	R ₁	R ₂	V _p	N _D	No.	Blank size	R ₁	R ₂	V _p	N _D
1	1	1	1	1	1	28	2	1	1	1	3
2	1	1	2	1	1	29	2	1	2	1	3
3	1	1	3	1	1	30	2	1	3	1	3
4	1	1	1	2	2	31	2	1	1	2	1
5	1	1	2	2	2	32	2	1	2	2	1
6	1	1	3	2	2	33	2	1	3	2	1
7	1	1	1	3	3	34	2	1	1	3	2
8	1	1	2	3	3	35	2	1	2	3	2
9	1	1	3	3	3	36	2	1	3	3	2
10	1	2	1	1	1	37	2	2	1	1	2
11	1	2	2	1	1	38	2	2	2	1	2
12	1	2	3	1	1	39	2	2	3	1	2
13	1	2	1	2	2	40	2	2	1	2	3
14	1	2	2	2	2	41	2	2	2	2	3
15	1	2	3	2	2	42	2	2	3	2	3
16	1	2	1	3	3	43	2	2	1	3	1
17	1	2	2	3	3	44	2	2	2	3	1
18	1	2	3	3	3	45	2	2	3	3	1
19	1	3	1	1	2	46	2	3	1	1	3
20	1	3	2	1	2	47	2	3	2	1	3
21	1	3	3	1	2	48	2	3	3	1	3
22	1	3	1	2	3	49	2	3	1	2	1
23	1	3	2	2	3	50	2	3	2	2	1
24	1	3	3	2	3	51	2	3	3	2	1
25	1	3	1	3	1	52	2	3	1	3	2
26	1	3	2	3	1	53	2	3	2	3	2
27	1	3	3	3	1	54	2	3	3	3	2

In addition, two different networks were developed with a single output to predict rolling load and torque. Schematic of the neural network structure established for rolling load and torque estimation based on the input parameters is shown in Fig 7. Moreover, a back-propagation algorithm (BPA) in MATLAB software was applied to develop ANN-based model. Back-propagation is a common technique of training artificial neural networks used in conjunction with an optimization method such as gradient descent. The present neural network is specified by major elements as follows [5]:

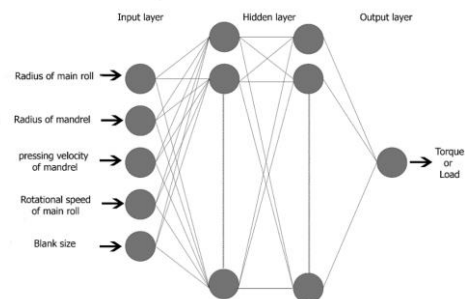


Fig. 7. Schematic model of the neural network construction

1. Its method of defining the weights on the connections, called the training algorithm. The fastest way for training moderate-sized feed-forward ANN is Levenberg–Marquardt back-propagation algorithm [5], which was implemented as training function here.
2. Its Transfer function which describe the relationship between the inputs and outputs of a system using a ratio of polynomials. Actually, transfer functions calculate a layer's output from its net input. Tensing and purelin are neural transfer functions which were used in the hidden and output layers, respectively.
3. Its net architecture which includes design of connections between the neurons, the arrangement of neurons into layers and the connection patterns within and between layers. In order to achieve optimal network architecture, the trial and

error method was used. In this paper, the best architecture of the network was achieved by trying different number of hidden layers and neurons. The objective was to increase correlation coefficient (R) to gain a network with the highest extension. Various network models were tried and their R values were computed. Several optimal created R values for different trials are shown in Table 5. The artificial neural network architecture and functions used in the resulted model are also summarized in Table 6. According to this table, the best R for both roll load and torque estimation was achieved by a network with two hidden layers have four and two neurons, respectively.

Table 5. Correlation coefficients (R) of ANN models for describing the best network architecture

no.	Neurons numbers in hidden layer 1	Neurons numbers in hidden layer 2	R of roll load prediction		R of roll torque prediction	
			train	test	train	test
1	3	-	0.99878	0.97327	0.99812	0.99855
2	4	-	0.99802	0.99739	0.99946	0.99914
3	6	-	0.99850	0.98862	0.99947	0.99565
4	8	-	0.99856	0.98484	0.99636	0.99583
5	14	-	0.99754	0.99263	0.99857	0.9842
6	17	-	0.99645	0.8868	0.97525	0.92656
7	4	4	0.99748	0.99469	0.98815	0.63713
8	4	1	0.99805	0.98902	0.9974	0.98713
9	4	2	0.99897	0.99826	0.99991	0.99933
10	5	4	0.99518	0.9863	0.96604	0.88191
11	5	3	0.99842	0.99139	0.9733	0.84252
12	5	2	0.99862	0.86403	0.99389	0.98208
13	6	6	0.92305	0.92628	0.96192	0.86708
14	6	4	0.99853	0.99426	0.9988	0.99408
15	6	3	0.9963	0.98785	0.98651	0.94775
16	7	5	0.96132	0.94986	0.99356	0.9859
17	7	3	0.99435	0.9458	0.98424	0.94456
18	7	1	0.9928	0.94374	0.9175	0.88236
19	8	4	0.9952	0.93519	0.99792	0.99249
20	8	2	0.95239	0.87528	0.94645	0.85873
21	11	8	0.97861	0.63602	0.97054	0.93732
22	11	6	0.99596	0.97053	0.99961	0.86265
23	12	7	0.98278	0.90435	0.99804	0.72665
24	12	5	0.98485	0.96957	0.98741	0.98612
25	14	10	0.99657	0.85372	0.99946	0.97485

Table 6. The architecture and functions of implemented ANN

Network	Feed forward backpropagation network
Training function	Levenberg–Marquardt
Learning function	Gradient descent with momentum weight and bias learning function
Transfer function	Tan sigmoid and Linear transfer function
Performance function	Mean squared error
Number of input layer unit	5
Number of hidden layers	2
Number of first hidden layer units	4
Number of second hidden layer units	2
Number of output layer units	1

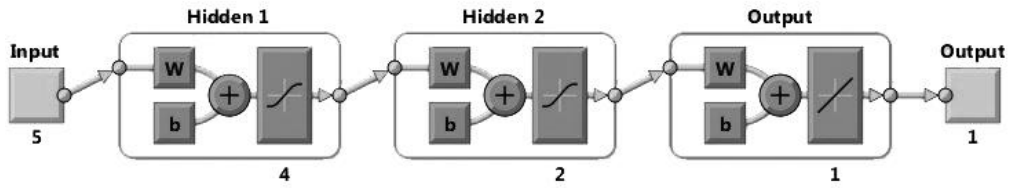


Fig. 8. View of the ANN in MATLAB software

The schematic of implemented neural network which was developed by MATLAB software is revealed in Fig.8

5. Genetic Algorithms

Genetic Algorithms (GAs) is a group of computational patterns inspired by development. Performance of GA starts with a population of chromosomes. After evaluation of the constructions, generative chances are assigns in a way that those chromosomes which demonstrate a better solution to the objective problem are given more chances to 'reproduce' than the others. The 'goodness' of a solution is generally defined with respect to the current population. Using MATLAB software, the modified GA was created. In order to detect the optimum input parameters which result into the lowest value of roll load and torque, the ANN-based model coupled with GA was also established in this study. Table 7 shows the specification of GA simulation Parameters.

Table 7. Parameters of GA simulation

Population size	80	
Reproducing (elite count)	4	
Fitness scaling (scaling function)	Rank	
Selection type	Tournament	
Cross over type	Two point	
Crossover fraction	0.8	
Migration fraction	0.2	
Mutation ratio	0.01	
Bounds of input parameters	lower	215, 250, 37.5, 0.5,35
	upper	304, 300, 55, 0.9, 60

6. Particle swarm optimization

PSO has been known as a population based technique, but instead of adopt a crossover or mutation operator, the search is performed through the adjustment of the velocity and location of a group of particles which move in the search area following one or more leaders. PSO is highly popular because of its simplicity and usefulness. PSO has been effectively applied in several areas such as: artificial neural network training, function optimization, fuzzy system control, and the other areas where GA is able to be used. The adjusted PSO was established by MATLAB software. In order to identify the optimum input parameters which result into the lowest value of roll load and torque, the ANN-based model coupled with PSO have also been developed in this research. Table 8 indicates the requirement of PSO Parameters.

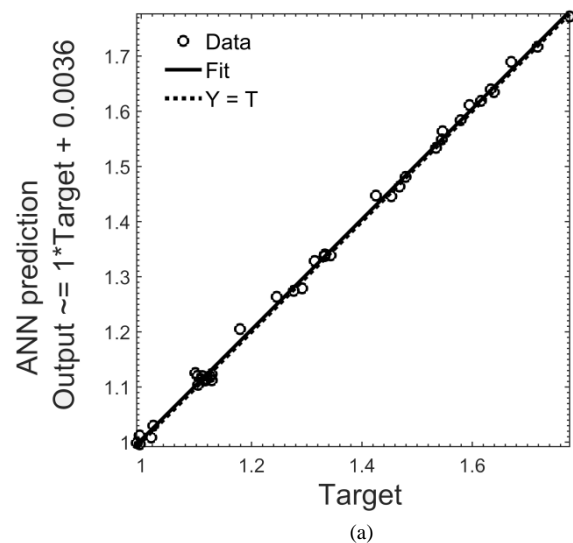
Table 8. Parameters of PSO simulation

Number of variables		5
Swarm size (Number of particles in the swarm)		30
Iteration		25
Hybrid Function		Fmincon (Find minimum of constrained nonlinear multivariable function)
Bounds of input parameters	lower	215, 250, 37.5, 0.5,35
	upper	304, 300, 55, 0.9, 60

7. Results and discussion

7.1. ANN results

The ANN model developed in this investigation is implemented to predict the rolling load and torque regarding 54 ring rolling process design outputs. Regression results of ANN for rolling load and torque are illustrated in Figs. 9 and 10. Apparently, appropriate prediction ability is achieved for training, validation, testing, and all data sets of rolling load and torque. Specifically, these results indicate that the present ANN is able to be used successfully for the objective system modeling. Moreover, the total performances of ANN model are estimated via method of mean square error (MSE) which are equal to 1.62×10^{-4} and 1.8×10^{-3} for rolling load and torque, respectively.



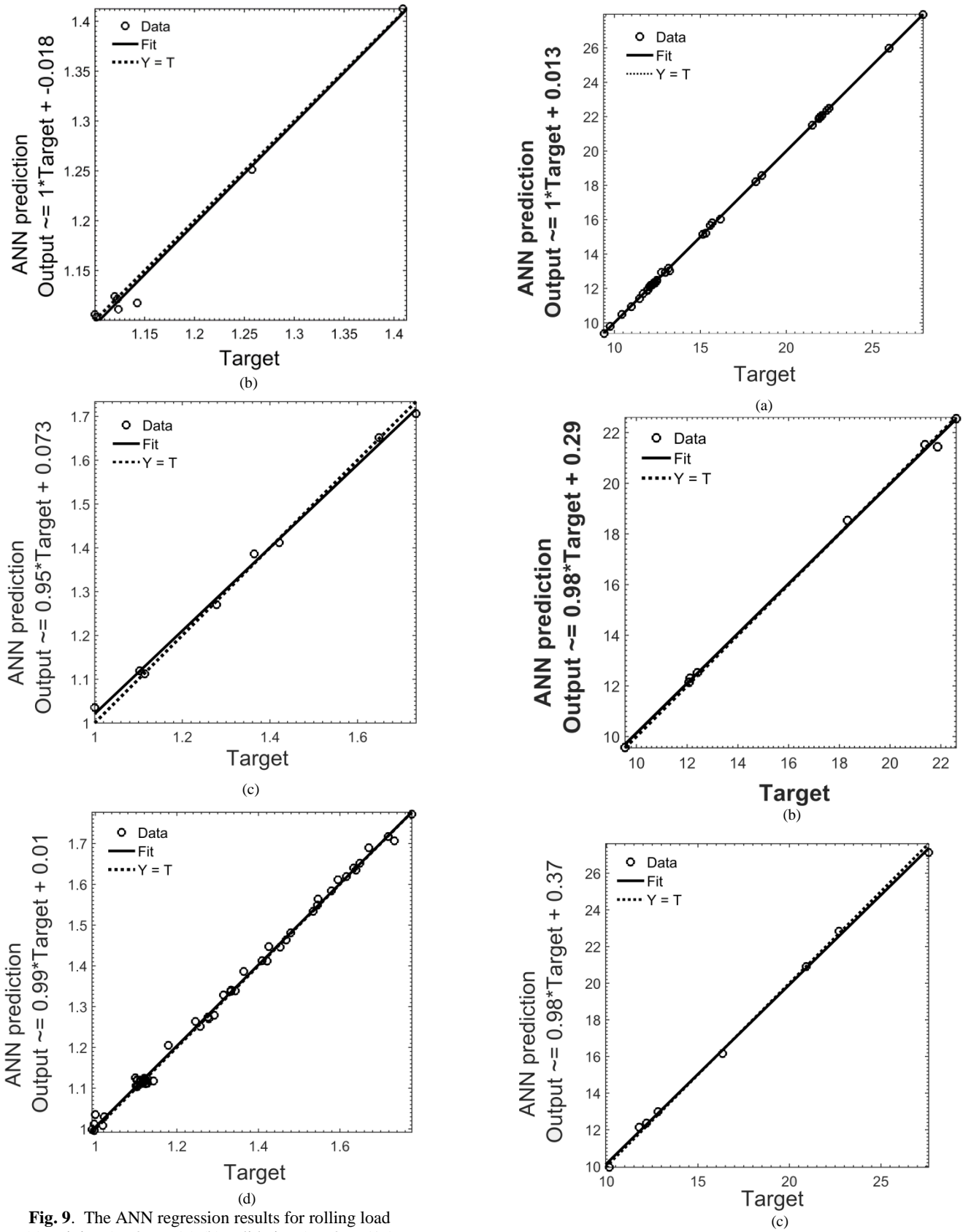


Fig. 9. The ANN regression results for rolling load (a) training (R=0.99957) (b) validation (R= 0.99519) (c) test (R=0.99284) (d) all (R=0.99824)

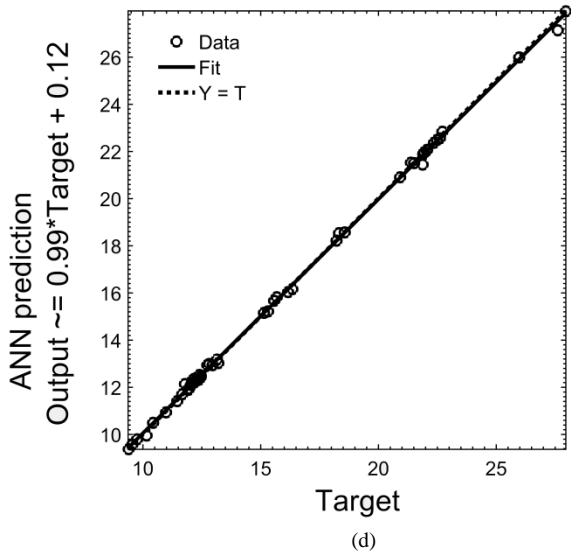


Fig. 10. The ANN regression results for rolling torque (a) training (R=0.99988) (b) validation (R= 0.99934) (c) test (R=0.99817) (d) all (R=0.99952)

The comparison between results predicted by developed ANN and target outputs concerning rolling load and torque are shown in Fig. 11. Furthermore, the error deviations of predicted rolling load and torque from real target values based on ANN are demonstrated in According to these figures, the present ANN can predict the rolling load and torque with a significant accuracy where the maximum errors in case of rolling load and torque are rarely higher than 0.3 and 4 % , respectively.

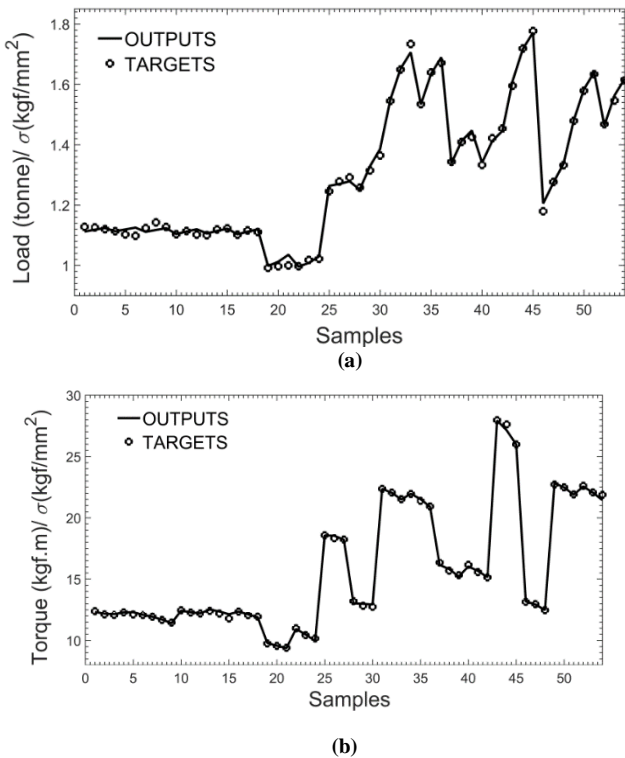


Fig. 11. Comparison between results predicted by developed ANN and target outputs for rolling (a) load (b) torque

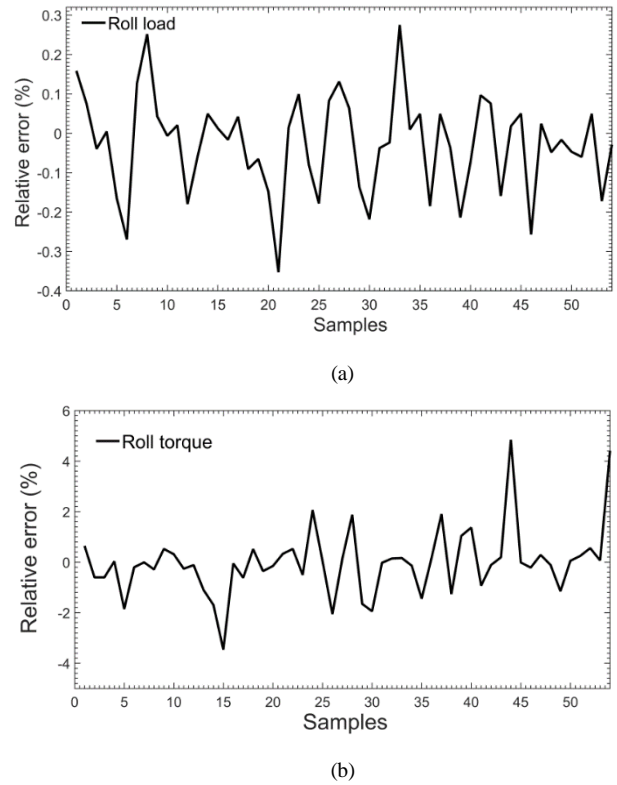


Fig. 12. Percentage error deviations of predicted rolling (a) load (b) torque

To investigate the fitness of established ANN, the network is tested using some known data which are out of range of the input parameters. In this case, the experimental results of [1] and [3] are considered. The results are presented in Fig. 13 where proper agreements between the results are noticeable.

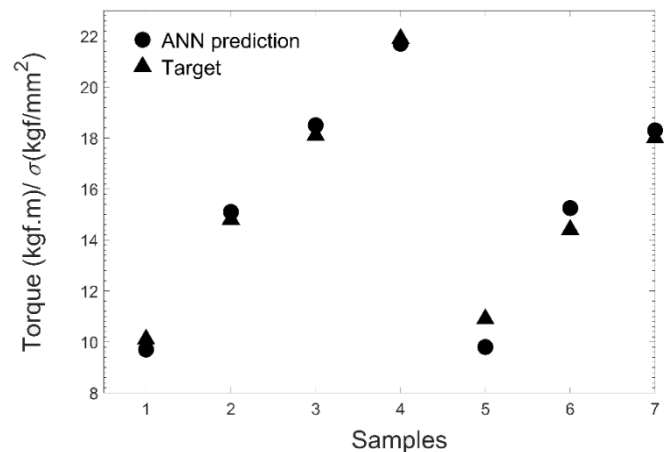


Fig. 13. Comparison of ANN prediction with target experimental results of [1]and [3][3]

Generally, the artificial neural network model is a complex nonlinear model, having several activation functions and interconnecting weights. Model response surfaces are able to achieve via varying two selected inputs, while all the remaining inputs are utilized at their nominal intermediate values. This model is an appropriate method to check the compatibility between the implemented models. It provides some indications on whether a

sufficient model has been implemented from the training data. Some usual response surfaces of the resulted ANN model, which indicate the rolling force and torque trends against two selected inputs are shown in Figs. 14 and 15.

These model response surfaces are able to provide the purpose of testing the reliability of the implemented models against existing process knowledge. Given in Fig. 14 (a), it is evident that the roll load significantly reduces whereas the radius of main roll increases. Conforming to the Fig. 14 (b), feed speed of the mandrel has considerable influence on the rolling load. It can be seen that the roll load rises dramatically as feed speed of mandrel soars. Regarding the Fig. 15 (a), torque increases rapidly when value of angular velocity and radius of mandrel increases. As it can be seen in Fig. 15 (b), increasing the feed speed results that the torque substantially rises.

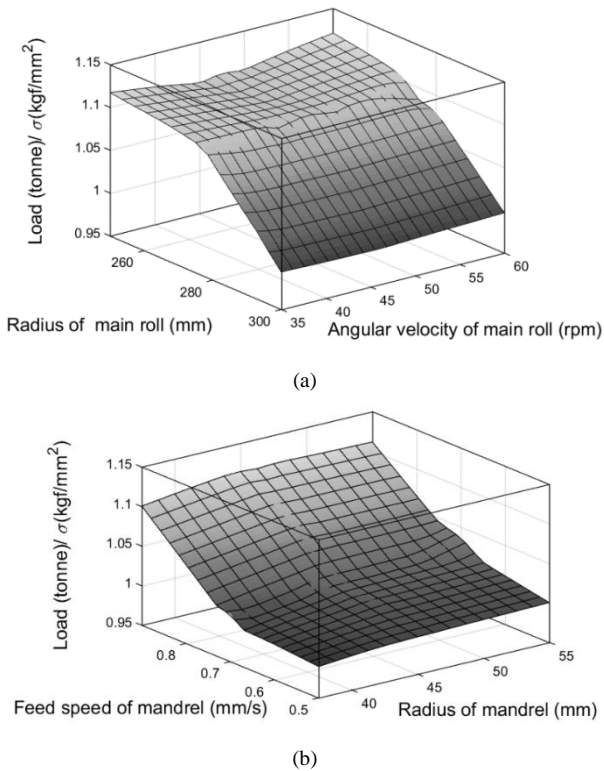


Fig. 14. Evolution of roll load vs. feed speed of mandrel and radius of (a) main roll (b) mandrel

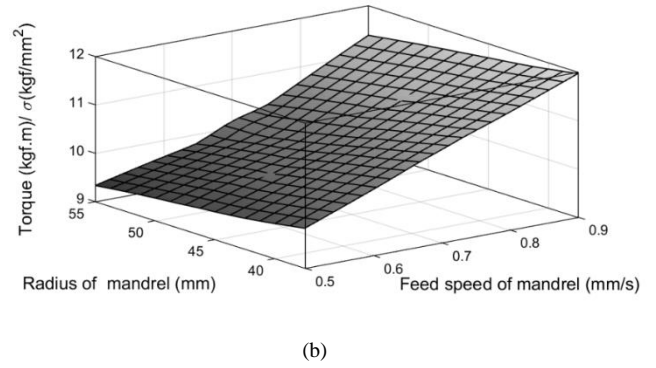
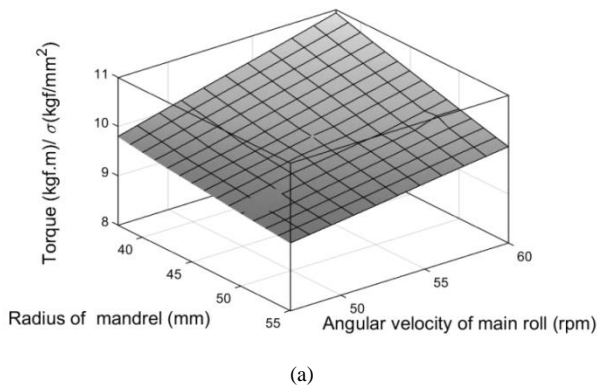
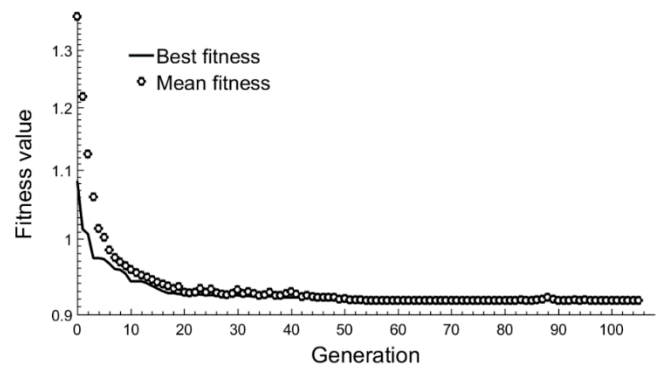


Fig. 15. Evolution of roll torque vs. feed

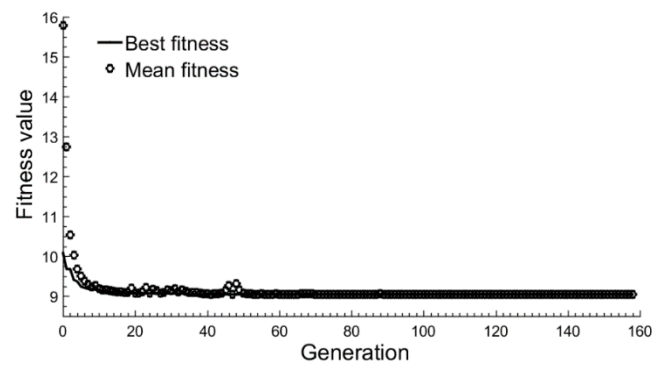
speed of mandrel and radius of (a) main roll (b) mandrel

7. 2. GA results

The input parameters of the network as well as the weights and biases achieved from the highest regression of the ANN were employed by the developed GA. In this way, the GA established a first generation whose outputs lie between the lower and the upper bounds of network outputs. The creation of next generations was repeated until the minimized output was obtained which was close to the identified one from the network. Hereafter, corresponding input parameters were obtained. The fitness functions which were achieved for optimal state of rolling load and torque are shown in Fig. 16. Moreover, the optimized parameters of ring rolling process resulted into the minimum rolling load and torque are given in Table 9. GA is able to find the fitness value in less than 1 minute, using the Core 2 Duo CPU 2.4 GHz.



(a)



(b)

Fig. 16. Evolution of the fitness function for optimal state of rolling (a) load (Best= 0.918098, Mean= 0.91805),

(b) torque (Best= 9.04403, Mean= 9.04449)

Table 9. Optimized parameters of ring rolling process

Parameter	Optimized value
Radius of main roll (mm)	299.84
Radius of mandrel (mm)	54.91
Rotational speed of main roll (rpm)	59.63
Pressing velocity of mandrel (mm/s)	0.502
Blank size (mm)	215×102×52

Table 10. Optimized parameters of ring rolling process

Parameter	Optimized value
Radius of main roll (mm)	300
Radius of mandrel (mm)	55
Rotational speed of main roll (rpm)	60
Pressing velocity of mandrel (mm/s)	0.5
Blank size (mm)	215×102×52

7.3 PSO results

Since PSO algorithm is required to initiate with generating the initial particles, ANN was applied as a function to assign the initial velocities. PSO calculates the objective function at each particle location and defines the best (lowest) function value as well as the best position. It chooses new velocities based on the current velocity, the particles' individual best locations, and the best locations of their neighbors. Then, it iteratively updates the particle locations, velocities, and neighbors. Actually, the new location is the old one plus the velocity, modified to keep particles within bounds. Iterations proceed until the algorithm reaches a stopping criterion. The cost functions that were reached for optimal state of rolling load and torque are illustrated in Fig. 17. In addition, the optimized parameters of ring rolling process resulted into the minimum rolling load and torque are provided in Table 10. Using the Core 2 Duo CPU 2.4 GHz, it was taken less than 10 seconds to simulate the process.

8. Conclusions

The current paper focuses on developing an ANN model to make a useful prediction about the ring rolling force and torque under various conditions with a substantial accuracy. Furthermore, optimal input parameters of the process are determined applying GA and PSO methods. In this regard, a three-dimensional finite element model of the process was established and approved using the experimental results of other investigators. Then, the data extracted from FE model was considered as a basis for training and validation of ANN. Next, a developed Levenberg–Marquardt feed-forward network was trained with BP algorithm and the optimum architecture was achieved by estimating the performance considering different number of hidden layers and neurons. It was shown that the ANN predictions have a significant conformity with the simulation and experimental outcomes. Hence, the developed model has an adequate precision to be used as a tool for prediction of ring rolling load and torque in different conditions. Finally, applying GA and PSO, the fitness function for optimum state of the process is obtained and optimal input process parameters lead to the minimum ring rolling load and torque are determined. Totally, based on finite element simulation, artificial neural network and optimization methods, the following conclusions are drawn:

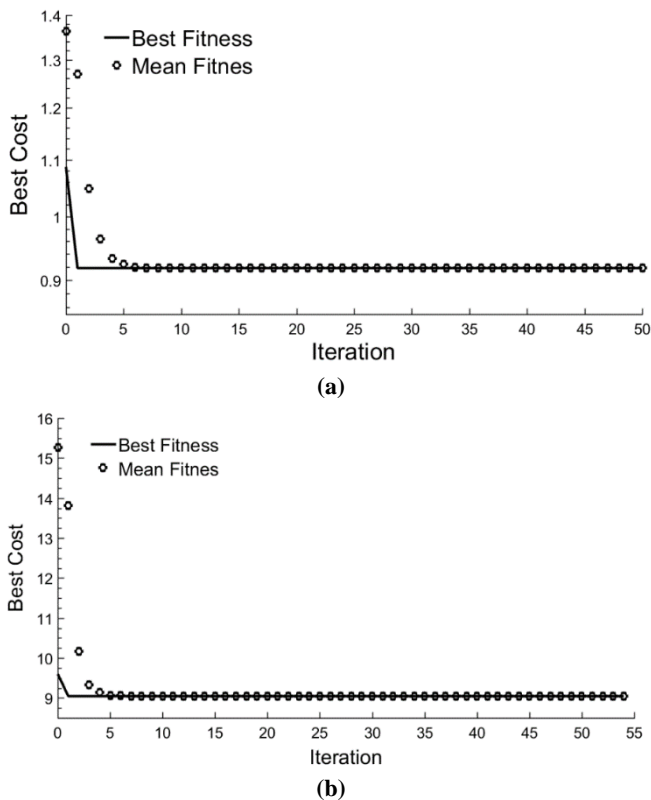


Fig. 17. Evolution of the fitness function for optimal state of rolling (a) load (Best= 0.918081) (b) torque (Best= 9.0441)

- Implemented Artificial Neural Network utilizing MATLAB software is able to put a reliable prediction on roll and torque values in ring rolling process.
- The present optimization techniques are capable to obtain the minimum roll and torque values in ring rolling process, reasonably.
- PSO accomplishes better results in a more efficient way compared with GA methods. Additional reason that PSO is more attractive is that there are fewer parameters to be adjusted.

Acknowledgments

The authors are grateful for the research support of the Iran National Science Foundation (INSF).

References

- [1] J. S. Ryoo, D. Y. Yang, W. Johnson, The influence of process parameters on torque and load in ring rolling, *Journal of Mechanical Working Technology*, Vol. 12, No. 3, pp. 307-321, 1986.
- [2] A. Parvizi, K. Abrinia, A two dimensional Upper Bound Analysis of the ring rolling process with experimental and FEM verifications, *International Journal of Mechanical Sciences*, Vol. 79, pp. 176-181, 2014.
- [3] D. Y. Yang, J. S. Ryoo, An investigation into the relationship between torque and load in ring rolling, *Journal of Engineering for Industry*, Vol. 109, No. 3, pp. 190-196, 1987.
- [4] G. Zhou, L. Hua, D. S. Qian, 3D coupled thermo-mechanical FE analysis of roll size effects on the radial-axial ring rolling process, *Computational Materials Science*, Vol. 50, No. 3, pp. 911-924, 2011.
- [5] L. Fausett, Fundamentals of neural networks: architectures, algorithms, and applications, *Prentice-Hall, Inc.*, 1994.
- [6] H. Altunkaya, I. E. I. M. Orak, Artificial neural network application for modeling the rail rolling process, *Expert Systems with Applications*, Vol. 41, No. 16, pp. 7135-7146, 2014.
- [7] M. Sharififar, S. A. A. Mousavi, Numerical study and genetic algorithm optimization of hot extrusion process to produce rectangular waveguides, *Journal of Computational Applied Mechanics*, Vol. 47, No. 2, pp. 129-136, 2016.
- [8] M. Moghaddam, F. Kolahan, An empirical study on statistical analysis and optimization of EDM process parameters for inconel 718 super alloy using D-optimal approach and genetic algorithm, *Journal of Computational Applied Mechanics*, Vol. 46, No. 2, pp. 267-277, 2015.
- [9] S. Jalilrad, M. H. Cheraghali, H. A. D. Ashtiani, Optimal Design of Shell-and-Tube Heat Exchanger Based on Particle Swarm Optimization Technique, *Journal of Computational Applied Mechanics*, Vol. 46, No. 1, pp. 21-29, 2014.
- [10] D. Y. Yang, J. S. Ryoo, J. C. Choi, W. Johnson, Analysis of roll torque in profile ring rolling of L-sections, *In: Proceedings 18th MTDR conference, London*, pp. 69-74, 1980.
- [11] G. I. Li, S. Kobayashi, Rigid-plastic finite-element analysis of plane strain rolling, *Journal of Engineering for Industry*, Vol. 104, No. 1, pp. 55-64, 1982.
- [12] C. C. Chen, S. Kobayashi, Rigid-plastic finite element analysis of ring compression, *Applications of Numerical Methods to Forming Processes*, Vol. 28, pp. 163-174, 1978.
- [13] G. R. Johnson, W. H. Cook, A constitutive model and data for metals subjected to large strains, high strain rates and high temperatures, *In Proceedings of the 7th International Symposium on Ballistic*, 1983.
- [14] S. P. F. C. Jaspers, H. Dautzenberg, Material behaviour in conditions similar to metal cutting: flow stress in the primary shear zone, *Journal of Materials Processing Technology*, Vol. 122, No. 2, pp. 322-330, 2002.
- [15] J. Deng, X. L. D. Gu, Z. Q. Yue, Structural reliability analysis for implicit performance functions using artificial neural network, *Structural Safety*, Vol. 27, No. 1, pp. 25-48, 2005.
- [16] R. Kazan, M. Firat, A. E. Tiryaki, Prediction of springback in wipe-bending process of sheet metal using neural network, *Materials & Design*, Vol. 30, No. 2, pp. 418-423, 2009.
- [17] B. Widrow, M. A. Lher, 30 years of adaptive neural networks: perceptron, madeline and backpropagation, *Proceedings of the IEEE*, 1990.